Crustal Deformation due to Atmospheric Pressure Loading in New Zealand

Research article

Vladislav Gladkikh, Robert Tenzer*†, Paul Denys

National School of Surveying, Division of Science, University of Otago, 310 Castle street, Dunedin, New Zealand

Abstract:

We investigate atmospheric pressure loading displacements in New Zealand using global and regional air-pressure data collected over a period of 50 years (1960-2009). The elastic response of the Earth to atmospheric loading is calculated by adopting mass loading Love numbers based on the parameters of the Preliminary Reference Earth Model (PREM). The ocean response to atmospheric loading is computed utilising a modified inverted barometer theory. The results reveal that the atmospheric loading vertical displacements are typically smallest along coastal regions, while gradually increasing inland with the maximum peak-to-peak displacement of 13.1 mm for this study period. In contrast, the largest horizontal displacements are found along coastal regions, where the maximum peak-to-peak displacement reaches 2.7 mm. The vertical displacements have a high spatial correlation, whereas the spatial correlation of the horizontal displacement components is much smaller. A spectral decomposition of the atmospheric loading time series shows that the signal is a broad band with most energy between 1 week and annual periods, and with a couple of peaks corresponding to approximately annual forcing and its overtones. The largest amplitudes in the atmospheric loading time series have an annual and semi-annual period.

Keywords:

Atmosphere • Correlation • Displacement • Loading • Pressure • Time series © Versita Warsaw and Springer-Verlag Berlin Heidelberg.

Received 2011-05-03; accepted 2011-06-03

1. Introduction

Displacementă of the Earth's surface and changes in the Earth's gravity field induced by surface loads are computed using the theory of Farrell (1972). According to his theory, the loading displacements are computed through the integral convolution of the surface load expressed by means of the surface pressure and with appropriate Green's functions. van Dam and Wahr (1987) were the first who utilised the method of Farrell (1972) in computing the atmospheric loading displacements using the local air-pressure data provided by the U.S. National Meteorological Center (NMC). They found that the peak-to-peak vertical displacements due to

atmospheric loading could be as large as 15 to 20 mm. They also observed that the displacements are generally larger at higher latitudes and during the winter season. Their results showed that taking only air-pressure variations in the vicinity of observation points into consideration is not sufficiently accurate for computing the atmospheric loading. Instead, the regional air-pressure data from at least the surrounding 1000 km are necessary (given the present level of the accuracy of geodetic measurements). The atmospheric loading displacements were detected from the analysis of VLBI and GPS data by MacMillan and Gipson (1994), van Dam and Herring (1994), and van Dam et al. (1994). Manabe et al. (1991) calculated the vertical atmospheric loading displacements for a number of VLBI stations using global air-pressure data provided by the Japanese Meteorological Agency Global Objective Analysis. Petrov and Boy (2004) presented a procedure for computing the 3-D crustal deformations due to atmospheric loading using the global air-pressure data (collected with a 6 hour sampling interval)



^{*}E-mail: Robert.Tenzer@otago.ac.nz, Phone: +64 3 479 7592, Fax: +64 3 479 7586

[†]corresponding author

provided by the National Centre for Environmental Prediction - National Centre for Atmospheric Research (NCEP/NCAR; formerly NMC) of the National Oceanic and Atmospheric Administration (NOAA). They compared the atmospheric loading time series with a data set of 3.5 million VLBI observations between 1980 and 2002. They also developed software for computing the displacements, and established an online Atmospheric Pressure Loading Service, where the loading time series for a large number of VLBI, SLR, GPS, and DORIS stations, as well as the atmospheric loading data with a global coverage on a 2.5×2.5 arc-deg geographical grid (updated daily) are made available since 1976.

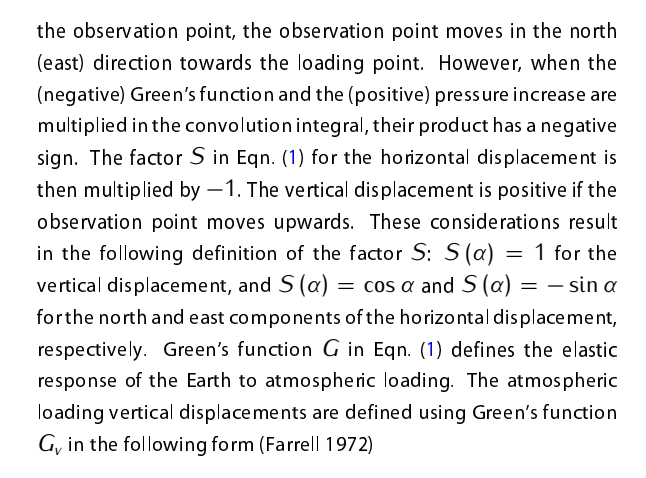
The analysis of atmospheric pressure loading as well as other timevariable signals due to ocean-tide loading, post-glacial isostatic adjustment, variations in the pole position, soil moisture, snow cover, etc. (cf. e.g., Heki 2004) is done in the context of various highaccuracy geoscience applications, such as the estimation of crustal displacements and absolute sea level rise using the continuous GPS and tide-gauge data. In this study, we compute and investigate atmospheric loading displacements in New Zealand. We note that the analysis of GPS and tide-gauge data corrected for the aforementioned signals will be addressed in a forthcoming study. The method of computing the atmospheric loading is briefly reviewed in Section 2. The input data description and the results of numerical analysis are shown and discussed in Section 3. In particular, we investigate the maximum crustal displacements due to atmospheric loading in New Zealand over the study period of 50 years, the spatial correlation of the horizontal and vertical displacements, and the spectral characteristics of the atmospheric loading signal. The summary and conclusions are given in Section 4.

2. Methodology

The crustal displacement u at a position (ϕ, λ) and time t is computed as the integral convolution of the atmospheric surface load μ and Green's function G in the following form (Farrell 1972)

$$u\left(\phi,\lambda,t\right) = \iint_{\Omega' \in \Omega_{0}} G\left(\psi\right) \, \mu\left(\phi',\lambda',t\right) \, S\left(\alpha\right) \, d\Omega', \quad (1)$$

where $d\Omega'=\cos\phi'\,d\phi'\,d\lambda'$ is the infinitesimal surface element on the unit sphere, and Ω_0 denotes the full solid angle. The 3-D position (r,ϕ,λ) is defined in the coordinate system of which the origin coincides with the solid Earth centre of mass as defined in Farrell (1972); r is the radius, and $\Omega=(\phi,\lambda)$ denotes the pair of spherical coordinates with the spherical latitude ϕ and longitude λ . The system of polar spherical coordinates (α,ψ) is described by the spherical distance ψ and azimuth α . The azimuth is measured counter clockwise from the southern direction. The north (east) horizontal displacement component is considered positive if the observation point moves in the north (east) direction. When there is an increase of pressure at a point located to the north (east) from



$$G_{\nu}(\psi) = \frac{R}{M} \sum_{n=0}^{\infty} h'_{n} P_{n} (\cos \psi). \tag{2}$$

The Green's function $G_{\rm h}$ for describing the corresponding horizontal displacements reads (ibid.)

$$G_h(\psi) = \frac{\mathsf{R}}{M} \sum_{n=1}^{\infty} \mathsf{l}_n' \frac{\partial P_n(\cos \psi)}{\partial \psi}. \tag{3}$$

In Eqns. (2) and (3), R is the Earth's mean radius, M is the total mass of the solid Earth (i.e., excluding the atmosphere and ocean), P_n are the Legendre polynomials of degree n for the argument of cosine of the spherical distance ψ , and h'_n and l'_n are the mass loading Love numbers defined for a particular model of the Earth (typically for the Preliminary Reference Earth Model (PREM); Dziewonski and Anderson 1981).

Farrell (1972) assumed that the loading mass distribution can be approximated by a thin layer at the Earth's surface. Guo et al. (2004) showed that this approximation also works for atmospheric pressure loading. They also calculated accurately the numerical values of Green's functions $G_{\rm v}$ and $G_{\rm h}$ adopted in this study.

When computing the atmospheric loading, the loading mass corresponds to the mass of the air-column at a position (ϕ', λ') and time t. The atmospheric surface load μ is then defined by (see e.g., Petrov and Boy 2004)

$$\mu\left(\phi',\lambda',t\right) = \frac{\delta P\left(\phi',\lambda',t\right)}{g_0},\tag{4}$$

where δP is the local variation of atmospheric pressure, and g_0 is the adopted mean value of gravity at the Earth's surface. Atmospheric pressure variations cause changes of the sea surface topography, which further deform the Earth's crust. We model the ocean response to the atmospheric pressure load variations using the theory of inverted barometer modified to account for the conservation of the oceanic mass (e.g., Petrov and Boy 2004, van Dam

et al. 1994). The standard inverted barometer theory is formulated based on the assumption that the sea surface depresses statically under the atmospheric pressure load by 1 cm for each 1 mbar of air-pressure exceeding the average air-pressure over the world ocean (Smith 1979, see also Lambeck 1980). Under this assumption, atmospheric pressure load variations at the ocean surface do not propagate through the ocean mass and consequently the ocean bottom surface does not experience any fluctuations in pressure loading. To account for a conservation of the total ocean mass, the inverted barometer theory is modified in the following way: If there is a net air-pressure change above the oceans, the ocean bottom surface at any point experiences the same pressure $\overline{\delta P}_0$ equal to the average variation of atmospheric pressure over the world ocean. Hence (e.g., van Dam and Wahr 1987)

$$\overline{\delta P}_{0}(t) = \frac{\iint_{\Omega' \in \Omega_{\text{Ocean}}} \delta P(\phi', \lambda', t) \ d\Omega'}{\iint_{\Omega' \in \Omega_{\text{Ocean}}} d\Omega'}, \quad (5)$$

where Ω_{Ocean} denotes the surface of the world ocean. Inserting Eqns. (4) and (5) to Eqn. (1), the loading integral is rewritten as (van Dam and Wahr 1987)

$$u\left(\phi,\lambda,t\right) = \frac{1}{g_0} \iint_{\Omega' \in \Omega_1 \text{ and }} G\left(\psi\right) \, \delta P\left(\phi',\lambda',t\right) \, S\left(\alpha\right) \, d\Omega'$$

$$+\frac{\overline{\delta P}_{0}(t)}{g_{0}}\iint_{\Omega'\in\Omega_{\text{Ocean}}}G(\psi)\ S(\alpha)\ d\Omega',\tag{6}$$

where Ω_{Land} denotes the total land surface. The loading integral in Eqn. (6) consists of the land and ocean surface terms. The relative magnitudes of these two terms depend on the distance of the observation point from the coastline and the coastline configuration. When the observation point is far from the ocean the first term in Eqn. (6) becomes dominant, and vice versa. The situation becomes more complicated at observation points located in the close proximity of the complex coastline due to the fact that temporal variations of these two integral terms might not correlate with each other. This is discussed in detail in Section 3.

According to both Chelton and Enfield (1986) and Ponte et al. (1991), the inverted barometer theory is likely to be a good approximation at periods of a few days to a few years. However, it does not describe the ocean response correctly over shorter time periods (van Dam and Herring 1994). Using polar motion data, Eubanks et al. (1985) concluded that the inverted barometer theory also may not work accurately in the southern ocean. We note that it is not yet known how well the inverted barometer theory is applicable to the region of New Zealand.

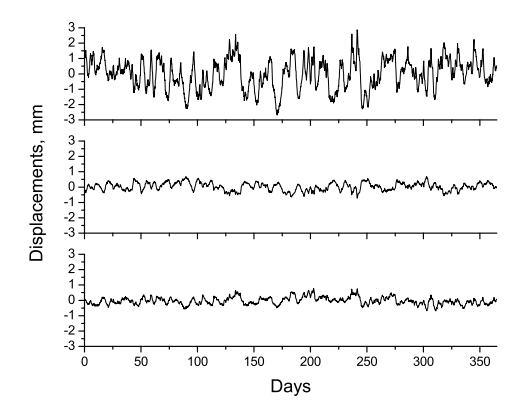


Figure 1. The atmospheric loading time series over the 1-year period of 2009 at the tide-gauge station in Dunedin. The displacement components: Vertical (top), North (middle), and East (bottom).

3. Numerical Analysis

To compute the near-zone contribution to atmospheric loading, we used air-pressure data generated on a 15 × 15 arc-min geographical grid within the study area of New Zealand (bounded by 34° -- 48°S and 166° -- 180° E) from the UV Atlas (version 2.2) compiled by the National Institute of Water and Atmosphere Research (NIWA). The air-pressure data product in the UV Atlas was prepared by Bodeker et al. (2006). We computed the far-zone contribution to atmospheric loading using the NCEP/NCAR global data of air-pressure with a spatial resolution of 2.5 × 2.5 arc-deg. The atmospheric loading was computed over the study period of 50 years (1960-2009) with a 6 hour sampling interval. The computation of the vertical and horizontal displacements was realised on a 5×5 arc-min geographical grid of points in New Zealand. In addition, the atmospheric loading time series were computed at the tidegauge stations in Dunedin, Lyttelton, Wellington, and Auckland. The variations of atmospheric pressure δP over the land surface in egn. (6) were calculated relative to the mean value of atmospheric pressure taken over the whole study period using the monthly global average NCEP/NCAR data. The example of the atmospheric loading time series over the 1-year period of 2009 at the tide-gauge station in Dunedin is shown in Fig. 1.

To analyze the spatial distribution of the largest variations in vertical and horizontal displacements, we computed the Root Mean Square (RMS) for each component of displacement u_{RMS} as follows

$$u_{RMS}(\phi,\lambda) = \sqrt{\frac{1}{N} \sum_{i=1}^{N} u^2(\phi,\lambda,t_i)},$$
 (7)

where $\{t_i: i = 1, 2, ..., N\}$, and N is the total number of time sampling data over the study period. The spatial distribution



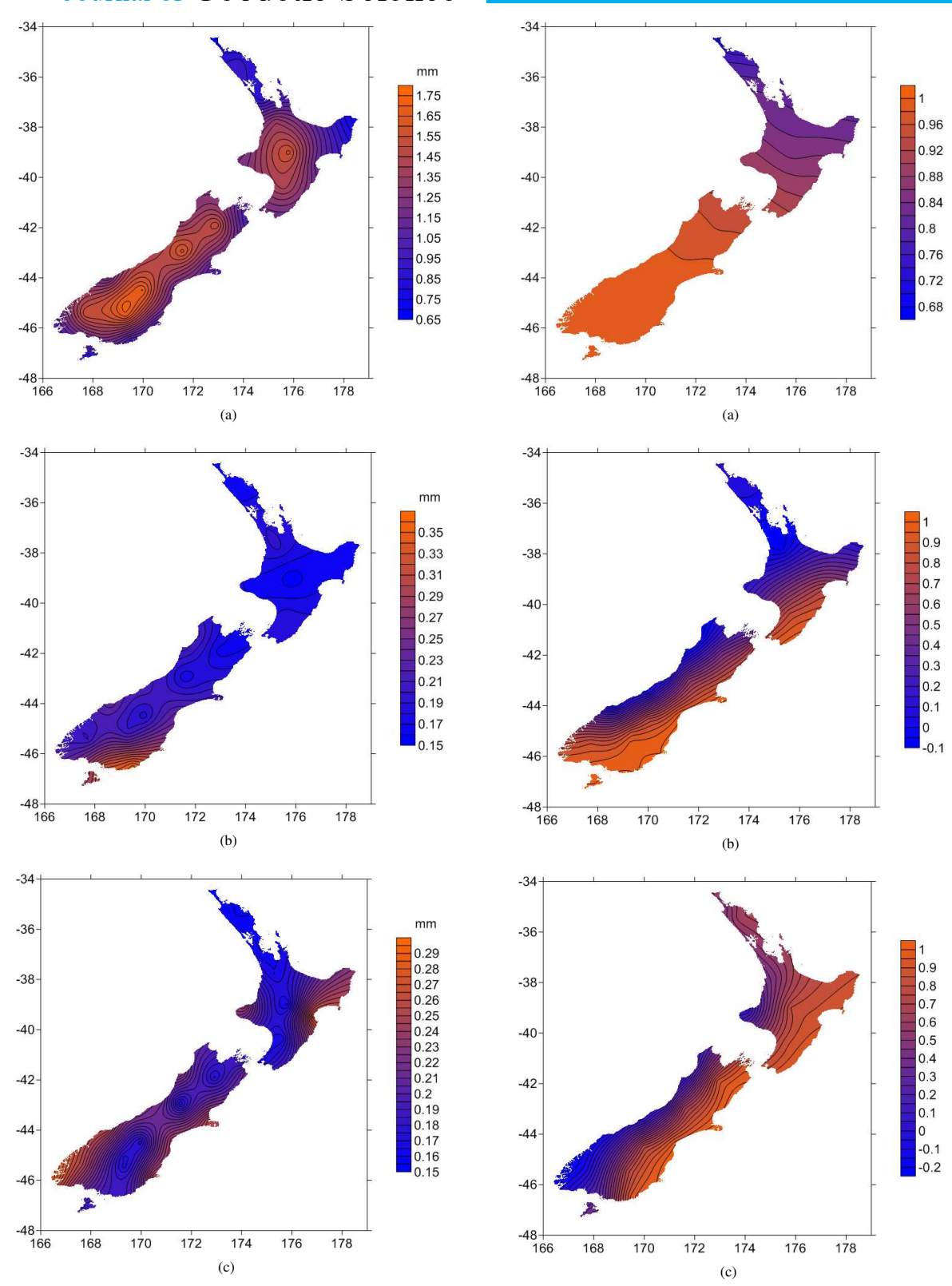


Figure 2. The RMS of atmospheric loading displacements in New Zealand over the study period: (a) Vertical, (b) North, and (c) East component.

Figure 3. The linear spatial correlation of atmospheric loading in New Zealand calculated relative to the atmospheric loading time series at the tide-gauge station in Dunedin: (a) Vertical, (b) North, and (c) East component.



of RMS values of the vertical and horizontal atmospheric loading displacements in New Zealand is shown in Fig. 2. The atmospheric loading displacements are defined positive in the upward, north, and east directions. The maximum range of vertical displacements reached 13.1 mm. The corresponding maximum range of horizontal displacements reached about 2.7 mm (for the north component) and 2.2 mm (for the east component). As seen from the spatial distribution of RMS values (in Fig. 2), the atmospheric loading vertical displacements are typically smallest along coastal regions, while gradually increasing inland. On the other hand, the largest horizontal displacements are found along coastal regions, with decreasing amplitudes inland. This can be explained by symmetry considerations. For a uniform (axially symmetric) air pressure change in the region of a site, the vertical displacement response has the same sign from each load component. At a near-coast site, where the ocean contribution to the load is reduced because of the inverted barometer response, the vertical response is less than if observed at an inland site. For a uniform (axially symmetric) air pressure change in the region of a site, the horizontal displacement response is zero, because the loads from opposite directions cancel out. At a near-coast site, the ocean loading contribution is less than the land contribution and hence there is a non-zero horizontal displacement response.

Given the theoretical framework in which we do this study, the loading signal is determined by two factors, namely the geographical distribution of atmospheric pressure and the coastline geometry. If the atmospheric loading signals at different sites are linearly correlated, it means that the atmospheric pressure distribution is the major factor. If this correlation is small, the geometry of coastlines plays a major role. The spatial correlation of atmospheric loading in New Zealand is demonstrated in Fig. 3, where the correlation of atmospheric loading at all observation points was calculated relative to the atmospheric loading time series at the tide-gauge station in Dunedin. The correlation of vertical displacements gradually decreases with an increasing distance (mainly in the south-north direction). The lowest correlation is at the upper North Island, where the linear correlation decreases to about 0.7. The spatial correlation of horizontal displacements has a different pattern. The large positive correlation along the east coast of the South and North Islands substantially decreases inland and even becomes negative along some parts of the west coast. The vertical displacements are thus highly spatially correlated, whereas the spatial correlation of the horizontal displacement components is much smaller. This demonstrates that the vertical displacements are mostly determined directly by the geographical atmospheric pressure distribution. On the other hand, the numerical values of the horizontal displacement Green's function G_h (in Eqn. 3) are smaller than the corresponding values of the vertical displacement Green's function G_v (in Eqn. 2), making the relative contribution of the coastline geometry more substantial. The horizontal responses on the east and west coasts are anti-correlated. This happens because when the load over the land is positive, coastal points will

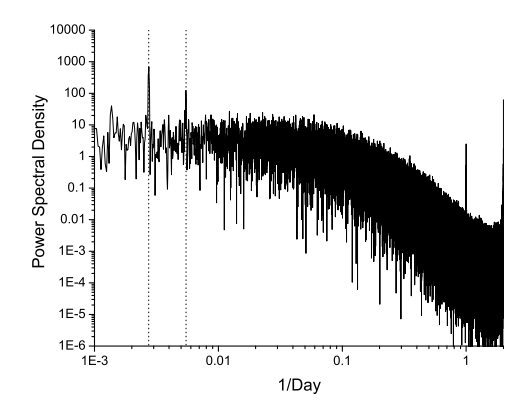


Figure 4. The power spectral density of the atmospheric loading time series (vertical component) at the tide-gauge station in Dunedin. Vertical dotted lines correspond to the annual and semi-annual frequencies.

be pulled inland towards the load. When the load over the land is negative, coastal points will be pushed away from the load.

We further computed the autocorrelation function and the power spectral density of the atmospheric loading time series. It is worth noting that the autocorrelation function provides information about the internal coherence of different parts of the signal, and the power spectral density gives the power per unit frequency interval. The example of a typical power spectral density, calculated at the tide-gauge station in Dunedin, is shown in Fig. 4. The power density increases with decreasing frequency with most of the energy distributed for wavelengths longer than 1 week. The power spectral density has four distinct peaks, corresponding to the semi-diurnal, diurnal, semi-annual, and annual oscillations. The amplitudes of these peaks differ from place to place. The spatial distribution of the semi-annual to annual peak ratio is shown in Fig. 5. This ratio is important because it determines the shape of characteristic oscillations in the autocorrelation function. The autocorrelation function of displacements decreases from 1 at t = 0 and then oscillates with the annual and semi-annual periods. The actual form of these oscillations is determined by relative amplitudes of the annual and semi-annual signals.

As seen in Fig. 5, the annual signal for the vertical and east displacements is stronger than the semi-annual signal (the semi-annual to annual peak ratio in the power spectral density function is everywhere <1). In contrary, the semi-annual signal for the north displacements has significantly higher amplitudes. We attribute this behaviour to the shape of New Zealand. Two examples of the autocorrelation functions computed at Lyttelton and North Cape are shown in Fig. 6. These locations were chosen where the semi-annual/annual peak ratio reaches its maximum (36.7) and minimum (0.8). In places where this ratio is small (<1), the north displacements oscillate similarly to the vertical and

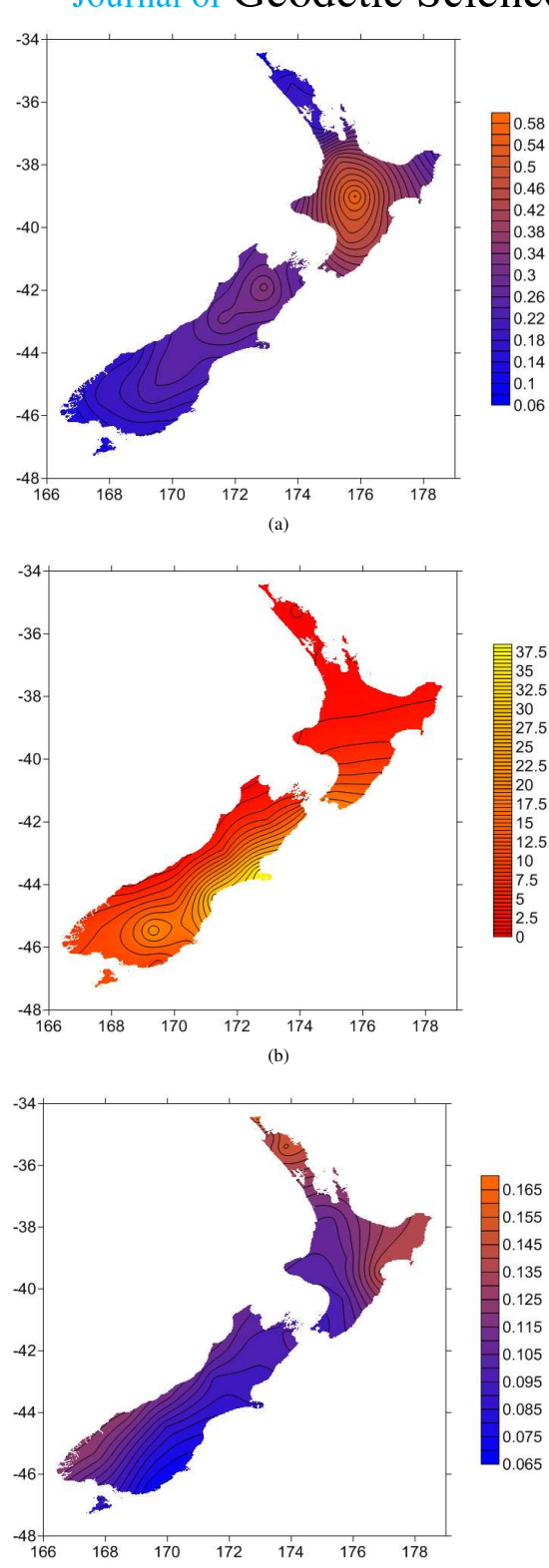
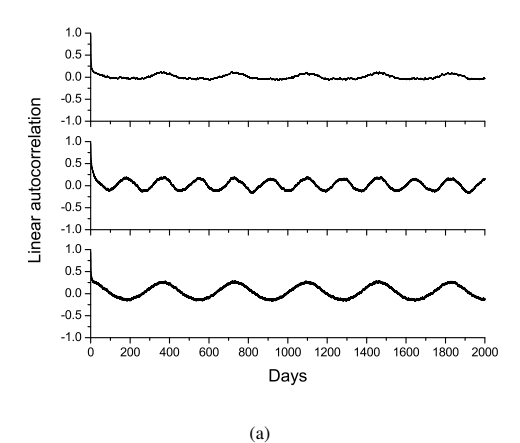


Figure 5. The spatial distribution of the semi-annual/annual peak ratio: (a) Vertical, (b) North, and (c) East component.

(c)





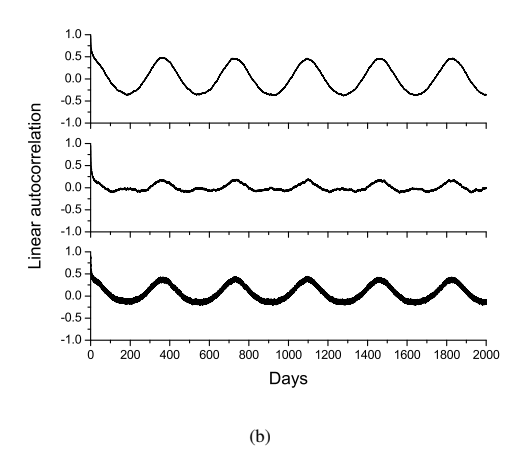


Figure 6. The linear autocorrelation coefficients of the atmospheric loading signal for (a) Lyttelton and (b) North Cape. The displacement components: Vertical (top), North (middle), and East (bottom).

east displacements with the presence of slight distortions. In places where this ratio is >1, the autocorrelation function of the north displacements oscillates twice as fast as the autocorrelation function of the vertical and east displacements. The annual and semi-annual signals are presented in the autocorrelation function and also as peaks in the amplitude spectra, because they are coherent from year to year. This means that their energy keeps adding to the same line in the spectrum.

The amplitude of oscillations of the autocorrelation function also differs from place to place. The spatial distribution of RMS values of the autocorrelation function is shown in Fig. 7. This amplitude has larger variations for the vertical component than the horizontal since the vertical displacements are influenced more by the ocean response to atmospheric loading (cf. also Fig. 9). As seen in the Fig. 7, the annual signal in vertical displacements is much more coherent in the upper North Island (narrow peninsula surrounded by the ocean).

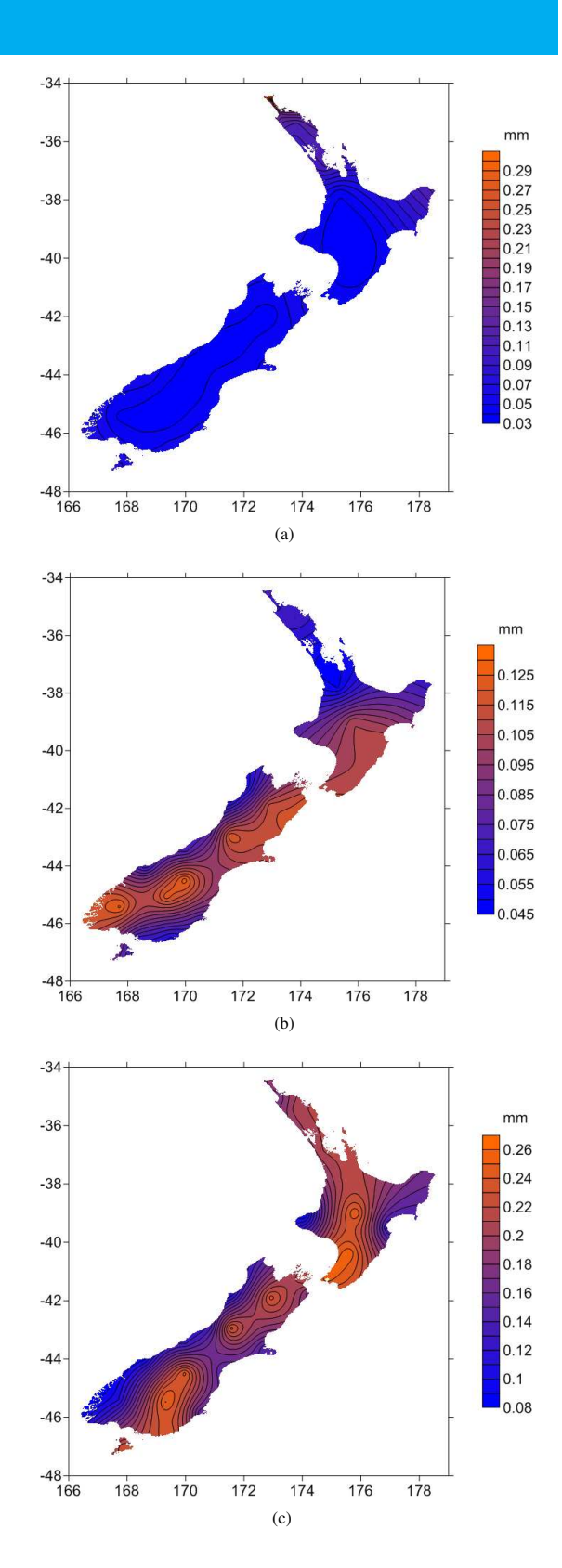


Figure 7. The RMS of the linear autocorrelation function of the atmospheric loading displacements in New Zealand over the study period: (a) Vertical, (b) North, and (c) East component.

1.0 0.6 0.6 0.2 0.2 0.2 0.4 0.0 600 800 1000 1200 1400 1600 1800 2000 Days

Figure 8. The linear autocorrelation coefficients of the oceanic part of the atmospheric loading signal.

Fig. 8 shows the autocorrelation function, when only the second (ocean surface) term in Eqn. (6) is taken into consideration. This function has only annual oscillations and has the same magnitude for all locations in New Zealand as well as for all three displacement components. The semi-annual peak in the corresponding power spectral density is much smaller than the annual one. From this we conclude that the differences in the total autocorrelation function from place to place are determined by the coastline geometry in the vicinity of observation points.

The ratio of RMS values of the land and ocean surface terms in Eqn. (6) is shown in Fig. 9. This shows the relative magnitudes of these two terms. The contribution of the land surface term is everywhere dominant. Moreover, the land-ocean term ratio for the horizontal displacements is larger than for the vertical displacements since the influence of the ocean term on the vertical displacements is stronger than on the horizontal ones.

4. Summary and Conclusions

We have investigated the atmospheric loading vertical and horizontal displacements in New Zealand over the period of 50 years (1960--2009) using the regional and global air-pressure data from the NIWA UV Atlas (version 2.2) and NCEP/NCAR of NOAA. The elastic response of the Earth to atmospheric loading was calculated using the mass loading Love numbers defined based on the PREM parameters, and the ocean response to atmospheric loading was computed using a modified theory of inverted barometer.

The maxima of the vertical atmospheric loading displacements were found in the central regions of the North and South Islands, whereas the corresponding maxima for the horizontal displacements are along coastal regions. The maximum peak-to-peak vertical and horizontal displacements in New Zealand over the study period reached 13.1 and 2.7 mm, respectively.

The vertical displacements have a high spatial correlation, while the spatial correlation of the horizontal displacements is much less pronounced. This phenomenon is explained by the large



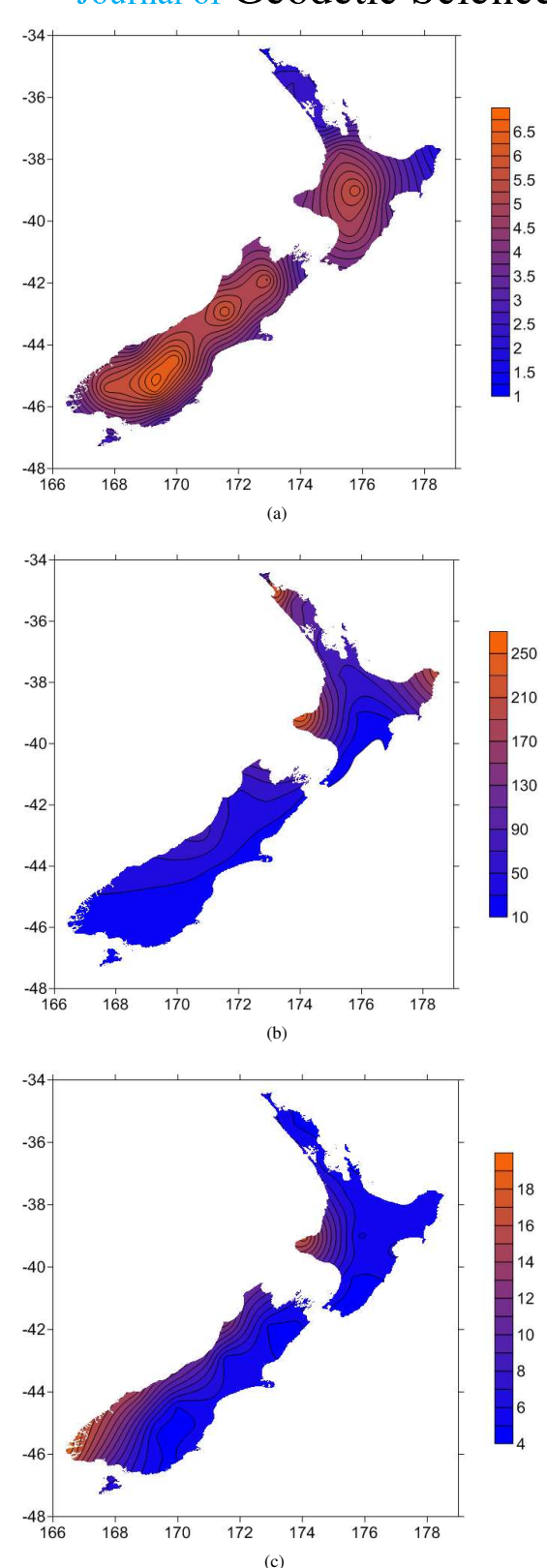


Figure 9. The ratio of RMS values of the land and oceanic terms in Eqn. (6): (a) Vertical, (b) North, and (c) East component.

VERSITA

dependence of the horizontal displacements on the coastal geometry. On the other hand, the vertical displacements are mainly characterized by the geographical air-pressure distribution.

The spectral decomposition of the atmospheric loading time series shows that the signal is a broad band with most energy between 1 week and 1 year periods, and with a couple of peaks corresponding to approximately annual forcing and its overtones. The largest amplitudes have an annual and semi-annual periods.

Acknowledgments

We thank Dr. Leonid Petrov (Goddard Space Flight Center, NASA) for a valuable discussion of computational methods. We thank Dr. Greg Bodeker for information regarding the sources and processing of regional air-pressure data in New Zealand. The air-pressure data used in this study are made available by the National Institute of Water and Atmospheric Research (NIWA) and the National Oceanic and Atmospheric Administration (NOAA). All results shown in this study were computed at the BlueFern High Performance Computing Facility of the University of Canterbury.

References

Bodeker G.E., Shiona H., Scott-Weekly R., Oltmanns K., King P., Chisholm H., McKenzie R.L., 2006, UV Atlas version 2: What you get for your money (Extended Abstract). UV Science Workshop organized by NIWA, Dunedin, April 19-21, 2006, RSNZ Miscellaneous Series 68. 102 p.

Chelton D.B., Enfield D.B., 1986, Ocean signals in tide gauge records. Journal of Geophysical Research - Solid Earth, 1986, 91(B9): 9081-9098.

Dziewonski A.M., Anderson D.L., 1981, Preliminary Reference Earth Model. Physics of the Earth and Planetary Interiors 25: 297-356.

Eubanks T.M., Dickey J.O., Steppe J.A., 1985, Rapid polar motions during 1984. Eos Trans. AGU 66, 854.

Farrell W.E., 1972, Deformation of the earth by surface loads. Reviews Geophysics and Space Physics, 1972, 10(3): 761-797.

Guo J.Y., Li Y.B., Huang Y., Deng H.T., Xu S.Q., Ning J.S., 2004, Green's function of the deformation of the Earth as a result of atmospheric loading. Geophysical Journal International, 2004, 159: 53-68.

Heki K., 2004, Dense GPS array as a sensor of for sea-

sonal changes of surface loads. In: State of the Planet: Frontiers and Challenges in Geophysics. (Ed.) Sparks R.S.J. and Hawkesworth C.J., American Geophysical Union, Washington, Geophysical Monograph Series 150: 177-196.

Lambeck K, 1980, The Earth's variable rotation: geophysical causes and consequences. Cambridge University Press, New York. 449 p.

MacMillan D.S., Gipson J.M., 1994, Atmospheric pressure loading parameters from very long baseline interferometric observations. J. Geophys. Res., 1994, 99(B9): 18081-18087.

Manabe S., Sato T., Sakai S., Yokoyama K., 1991, Atmospheric loading effect on VLBI observations. In: Proceedings of the AGU Chapman Conference on Geodetic VLBI: Monitoring Global Change, NOAA Tech. Rep. NOS 137 NGS 49. Pp. 111-122.

Petrov L., Boy J-P., 2004, Study of the atmospheric pressure loading signal in VLBI observations. J. Geophys. Res., 2004, 109, B03405.

Journal of Geodetic Science

Ponte R.M., Salstein D.A., Rosen R.D., 1991, Sea level response to pressure forcing in a barometric numerical model. Journal of Physical Oceanography, 1991, 21:1043-1057.

Smith N.P., 1979, Meteorological forcing of coastal waters by the inverse barometer effect. Estuarine and Coastal Marine Science, 1979, 8: 149-156.

van Dam T.M., Wahr J.M., 1987, Displacements of the Earth's surface due to atmospheric loading: Effects on gravity and baseline measurements. J. Geophys. Res., 1987, 92: 1281-1286.

van Dam T.M., Herring T.A., 1994, Detection of atmospheric pressure loading using very long baseline interferometry measurements. J. Geophys. Res., 1994, 99: 4505-4518.

van Dam T.M., Blewitt G., Heflin M.B., 1994, Atmospheric pressure loading effects on Global Positioning System coordinate determinations. J. Geophys. Res., 1994, 99: 23939-23950.